

Performance Analysis and Comparison of Three IPMSM with High Homopolar Inductance for Electric Vehicle Applications

Hussein Dogan, *IEEE Student Member*, Frédéric Wurtz, *IEEE Member*, Albert Foggia, *IEEE Life Senior Member*, Lauric Garbuio
Grenoble Electrical Engineering Laboratory
(G2ELab) Ense³ (Grenoble INP-UJF, CNRS UMR5529)
BP 46F – 38402 Saint Martin d’Hères, France
hussein.dogan@g2elab.grenoble-inp.fr ; frederic.wurtz@g2elab.grenoble-inp.fr ;
albert.foggia@g2elab.grenoble-inp.fr ; lauric.garbuio@g2elab.grenoble-inp.fr

Acknowledgements

The authors would like to thank the French automotive cluster *Mov’eo* for supporting the project *SOFRACI* of this work, and the industrial partners *Valeo* and *Leroy-Somer*.

Keywords

Permanent Magnets Synchronous Motor, Zero-Sequence Inductance, Electric Vehicle, Ripple Torque, Fast evaluation, Harmonics.

Abstract

This paper presents a comparison of different permanent magnets synchronous motors (PMSM) having a high homopolar or zero-sequence inductance. The high value of zero-sequence inductance is particularly a necessity for certain applications in which the winding coupling is not in Wye connection. Thereby, the homopolar currents which are sources of losses are reduced and minimized. In this study, we investigate three topologies of PMSM according to the specifications of an electric vehicle (EV) with severe constraints and a maximum rotation speed of 12, 000 rpm. Those fractional-slots machines are the 3-phase 12 slots / 8 rotor poles (12/8), the 12/10 and the 18/10. Then, the goal is to compare and evaluate the topologies firstly with a fast and coarse approach and then with finite element analysis (FEA) to finally determine which is the most suitable for the application.

1 Introduction

Due to the use of permanent magnets in the rotor, PMSM have the highest power density and efficiency among all types of motors. Therefore, PMSM have found wide attention in designing machines for a lot of high performance industrial applications and especially for hybrid electric vehicle (HEV) and electric vehicle (EV). Moreover, interior permanent magnet synchronous machines (IPMSM) are suitable for traction, thanks to their flux-weakening capability allowing wide-speed operation and high overload capability [1], [2]. Finally, fractional-slots machines having a fractional number of slots per pole per phase allow obtaining a smooth torque and a better fault-tolerant capability [3].

In embedded applications, fault tolerant is a key point for the designer. Thus, in order to minimize the fault between phases, phases should be electrically and magnetically separated. The magnetic separation is accomplished when the mutual inductances are as low as possible [3], [4], meaning a high value of the zero-sequence inductance. Furthermore, the high value of the homopolar inductance is also a requirement for certain power supply structure and when the winding coupling is in Δ connection in order to diminish homopolar currents, which are inexistent when the winding coupling is in Wye [5].

In this work, we aim at designing a machine fulfilling the specifications of an original electric drive dedicated to the vehicle traction [6], patented by a French automotive OEM *Valeo* [7]. This electric drive has the great advantage of being configurable as a battery charger without need of additional components. Moreover, it allows a high charging power for short duration charge cycles [8] and a higher efficiency than traditional 3-leg inverter [6]. Finally, since that each phase is fed by a full-bridge converter, the electric separation among the phases is also realized [3]. However, because of the 3H-Bridge inverter [6], this topology, as shown in Fig. 1, requires a high value of the zero-sequence inductance in order to minimize homopolar currents. Indeed, at high speed and in flux-weakening region, i.e. around 12,000 rpm, zero currents resulting from harmonics multiple of 3, principally the 3rd harmonic, could be very elevated and induce important losses not only in the motor but also on the electronic parts of the power supply [9].

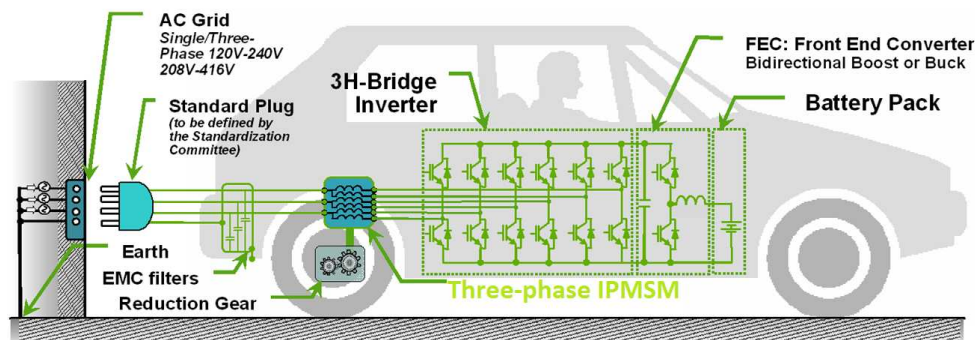


Fig. 1: Power supply of the PMSM: 6-leg voltage source inverter (VSI) [7]

Ultimately, the purpose of this paper is to study and determine the most favorable slots/pole combination and its winding arrangement among three different candidate machines. The specifications impose combination of high performance, i.e. high power density, high efficiency and low values of harmonics, principally 3rd, 5th and 7th harmonics, and high value of phase inductance and homopolar inductance.

Thus, in section 2, the main design considerations for the choice of the right machine are introduced. A first assessment of the performance of the machines is also given by the observation of the winding function, the slots-poles combination and the zero-sequence inductance ratio. Then, results of the simulation from FEA of the three PMSM are presented and compared in section 3. The comparisons include the different characteristics as torque, synchronous, self, mutual and zero-sequence inductances, iron and eddy-current losses, back-emf and harmonics. Finally, in section 4, proposition of solutions to the drawbacks of each machines is given and selection of the more suitable machine for this application is also studied.

2 Design considerations

2.1 Ripple torque and cogging torque

The literature presents three sources of torque ripple coming from the machine [10]:

1. Cogging torque
2. Difference between permeances of the air gap in the d- axis and q- axis (reluctance torque)
3. Distortion of the magnetic flux density waveform in the air gap

The cogging torque comes from the interaction of the permanent magnets located in the rotor with the stator teeth. When the rotor moves relatively to the stator, we obtain a variation of the air gap reluctance which has a minimum value in front of a tooth and a maximum value in front of a slot. Thus, the rotor tends to move naturally toward the position(s) minimizing the reluctance of the circuit.

Obviously, the slots/poles combination has a direct influence on the cogging torque and an overview of the torque ripple can be done once the topology is determined. This is obtained by the greatest common divisor (GCD) and the least common multiplier (LCM) between the N_s slots and p poles. In

fact, the machine periodicity and also the first harmonic of the cogging torque are done by the greatest common divisor (LCM). Then, the LCM should be the greatest possible in order to reach a low value of the cogging torque. For the GCD, it is the opposite reasoning. Smaller is the GCD, lower will be the ripple torque [10]. However a small value of GCD is synonymous of unbalanced radial forces and magnetic noises. Then, another way to lessen these undesired forces is to have an even value of the GCD. [11] consider that the GCD should be an even number and as high as possible, since this indicates more radial symmetry, good force balance, and higher vibration modes of the machine. Therefore, there is a compromise between the value of the cogging torque and the radial forces.

Considering table I, it can be observed that the 12/10 and 18/10 machines have a high value of LCM and a low value of GCD. This expects a low value of the ripple torque but a riskiness of unbalanced forces. Likewise, the 12/8 has good balanced radial forces but could have high value of ripple torque.

Table I: GCD and LCM of the three machines

Topology (N_s/p)	GCD	LCM
12/8	4	24
12/10	2	60
18/10	2	90

2.2 Star of slots

As explained in [3], [12] and [13], the star of slots or coil-EMF vectors [14] allows determining the right coils connections in order to realize a valid machine winding. There are also some rules in the right choice of the corresponding coil-EMF [12]. The first step is to determine the electric angle α_{es} between two consecutive slots. For a machine of N_s slots, α_{es} results in:

$$\alpha_{es} = \frac{2\pi}{N_s} \quad (1)$$

Then, star of slots can be drawn for each machine considered in this study. Figure 2 shows the representation of the coil-EMF vectors of each slot of the three machines:

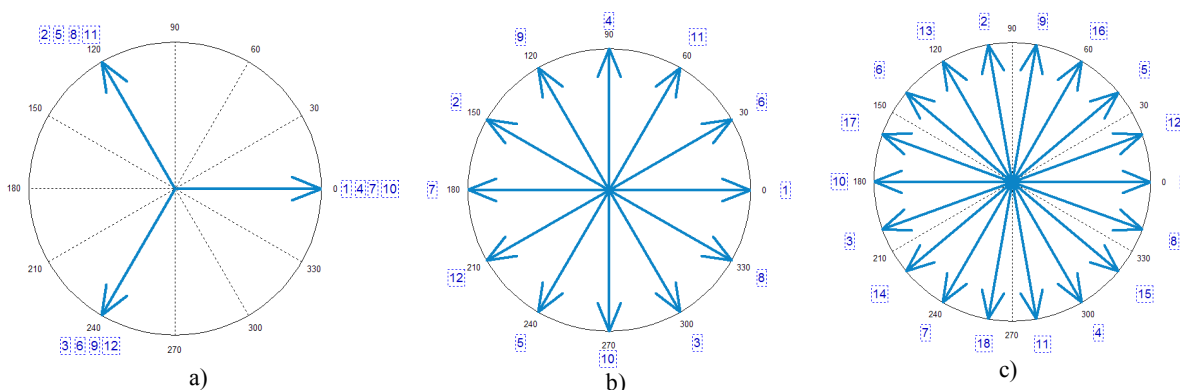


Fig. 2: Coil-EMF vectors of the machines: a) 12 slots / 8 poles, b) 12/10 and c) 18/10

The second step consists in choosing the slots for each phase which the coils will be wound. In general, this choice is realized by considering the maximization of the main harmonics of the EMF induced. In this study, the high value of the zero-sequence inductance is a key point. Thus, the choice has been realized by considering the maximization of this homopolar inductance. The method for determining the ratio of the zero-sequence inductance with the self inductance from each winding configuration is fully demonstrated in [9]. An instance is also given in zero-sequence inductance part.

Besides, the three machines are wound with a double-layer winding. Figure 3 illustrates the three machines with their respective winding configuration. Due to the periodicity which is two for the three cases, the representation of only half of the machines is sufficient. The symmetry is even for the 12/8 and odd for the 12/10 and the 18/10:

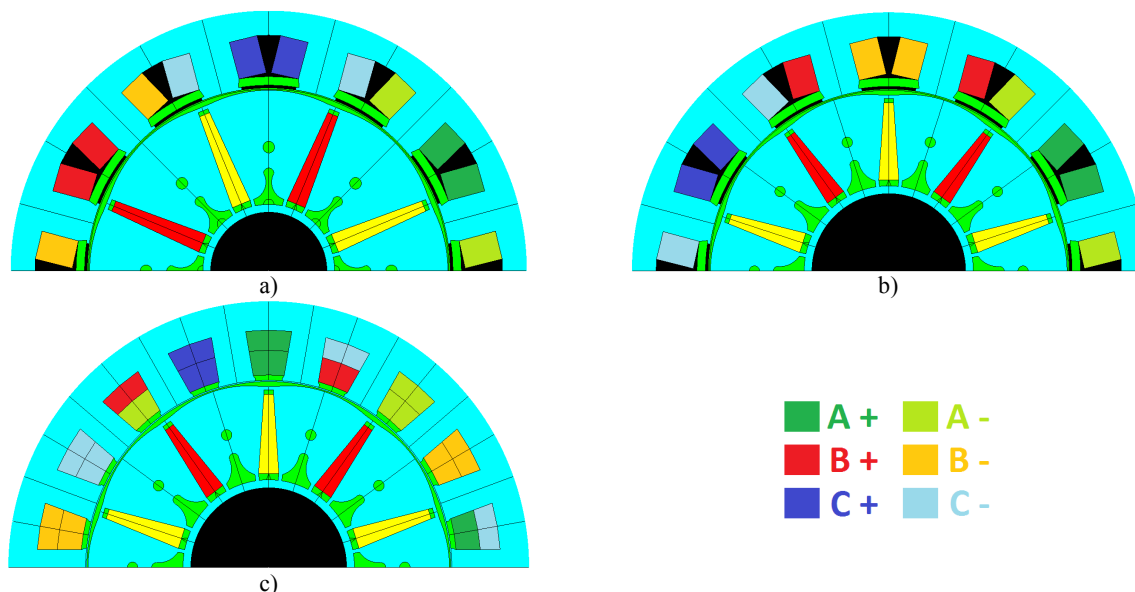


Fig. 3: Winding configurations of the three machines: a) 12/8, b) 12/10 and c) 18/10

Furthermore, [12] demonstrates that the star of slots could be used in determining the main harmonic winding factor and also the harmonics and sub-harmonics winding factors, since it contains information of the winding distribution, the harmonics content of the EMF waveform and the air-gap MMF distribution. However, the procedure is quite long and another known method using the winding function allows obtaining quickly the air-gap MMF distribution.

2.3 Winding function

Winding function can be used to calculate and evaluate several characteristics of the machines. Hence, it is possible to get quickly a first approach of the machine without employment of FEA. Moreover, the harmonic spectrum shows the values of harmonics and sub-harmonics which are very important to know in order to predict the presence of eddy-current losses in the magnets. In fact, the winding function corresponds simply to the MMF waveform in the air-gap when only one phase is fed by a positive current. In the following, the winding functions of the three machines are illustrated in figure 4 and an analysis of the harmonics is also given for each of them:

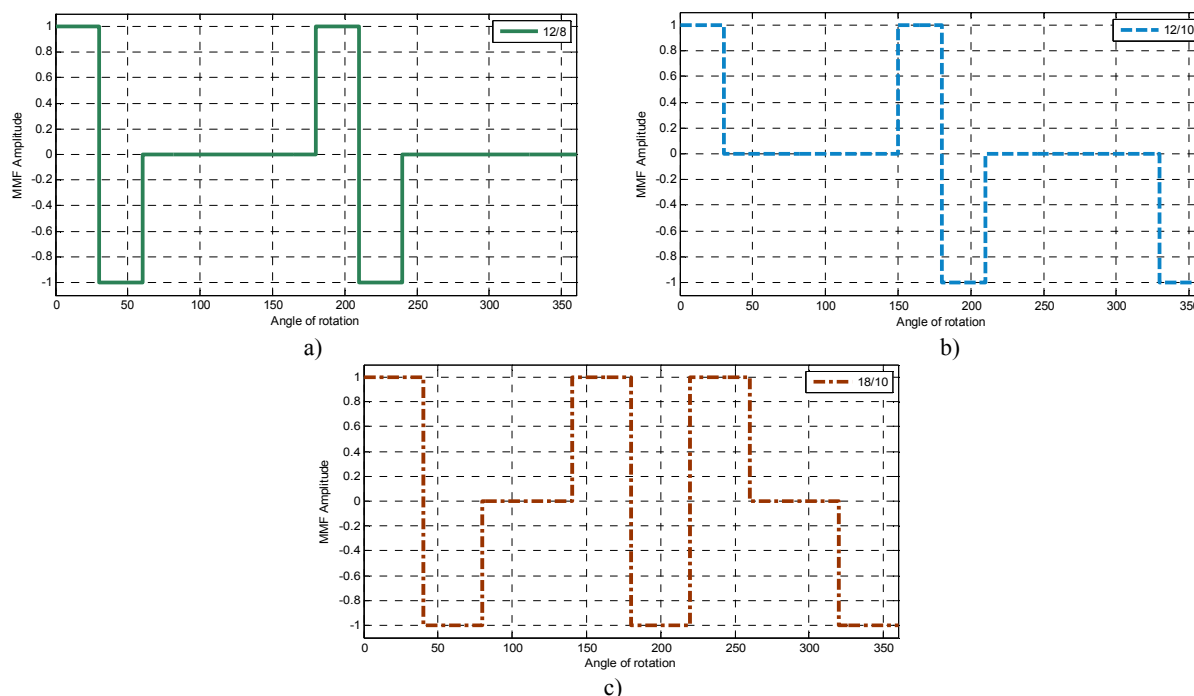


Fig. 4: Winding functions of the three machines: a) 12/8, b) 12/10, and c) 18/10

Evenly, the harmonics spectrums of the winding functions are shown in figure 5:

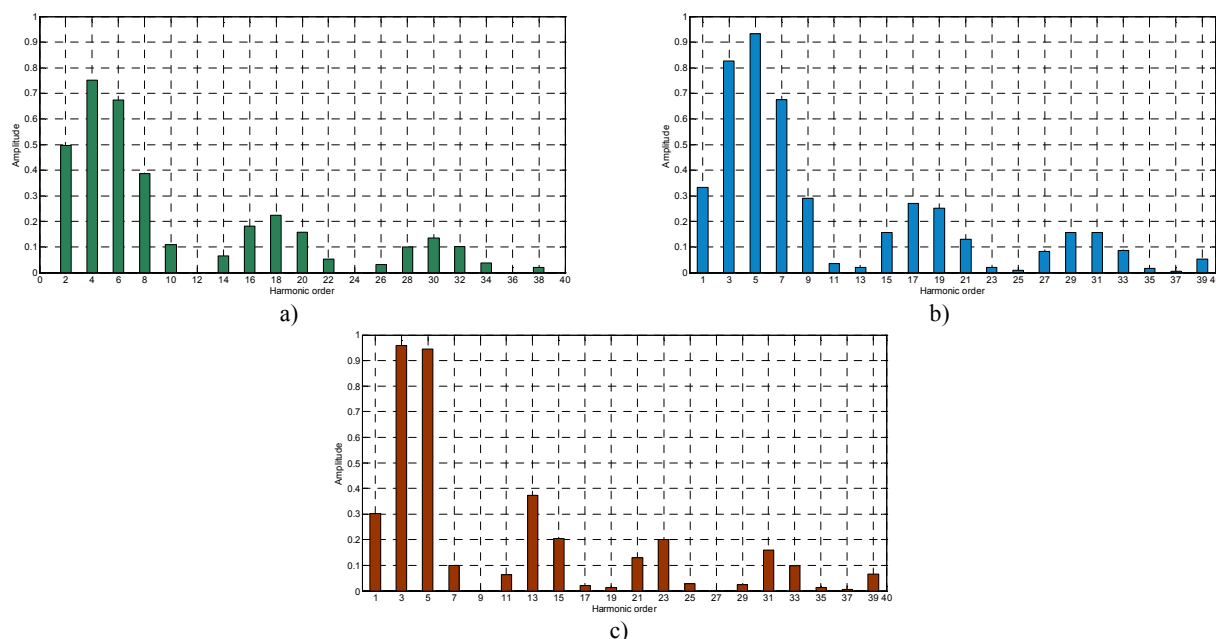


Fig. 5: Harmonic spectrum of the winding functions of the machines: a) 12/8, b) 12/10, and c) 18/10

First of all, the referential used for the harmonic spectrum is the mechanical (mech.) one. Thus, considering fig. 4 a), the electrical (elec.) fundamental corresponds to the 4th mech. harmonic because of the number of pole pairs. Then, from the harmonic spectra of the winding function, several deductions could be done as:

- Winding factors
- Subharmonics
- Presence or not of the zero-sequence inductance

The winding factors are important parameters to know since the fundamental component traduce the torque density, and the others, i.e. principally 3rd, 5th and 7th elec. components are sources of undesirable effects. In traditional Wye winding connection, the EMF induced in the windings from the components multiple of 3 is null. However, with other winding connections and especially with the structure studied in this paper, the EMF induced is not null and homopolar currents are expected. Evenly, having high values of 5th and 7th order harmonics could increase the torque ripple and induce harmonic components on the EMF induced. Hence, high value of the 1st order harmonic and low values of the 3rd, 5th and 7th order harmonics will be searched.

Besides, harmonics and inter-harmonics, being harmonic components with non-integral multiples of the fundamental, have as well adverse effects on the performance of the machines. Some of them rotate with a negative celerity and other rotate with a positive celerity. The literature demonstrates that for three phase machines with a sinusoidal current:

- Harmonic components as $h = 3j - 1$ ($j \in \mathbb{N}$) generate MMF waves rotating with an angular speed of $-\omega_e/h$ (ω_e is the electrical pulse)
- Harmonic components as $h = 3j + 1$ ($j \in \mathbb{N}$) generate MMF waves rotating with an angular speed of $+\omega_e/h$
- Harmonic components as $h = 3j$ ($j \in \mathbb{N}$) give a MMF which the sum is equal to zero

Consequently, asynchronous MMF waves, generating iron and eddy-current losses, will be created in the machine. Due to the lamination of the rotor and stator steels, these losses are considerably reduced. However, if the magnets are not segmented, which is the general case, high eddy-current losses can be predicted. [15] Demonstrates that the most responsible of the eddy-current losses induced in the magnets of the rotor are the subharmonics. These harmonics being components lower than the

fundamental have higher wavelength and higher rotational speed compare to the main harmonic. As a consequence, flux lines penetrate deeply into the rotor. Therefore, low values of subharmonics (being not multiple of 3 with the mech. referential) will give better performances.

Furthermore, considering 3-phases machines, the zero-sequence inductance exists only with the presence of certain harmonics. The MMF induced in the machine for the phases A , B and C are:

$$\begin{cases} MMF_A(\theta) = NI \cdot \cos(\theta) + NI \cdot \sum_{n=2}^{\infty} \cos(n\theta - \varphi_A(n)) \\ MMF_B(\theta) = NI \cdot \cos(\theta - \frac{2\pi}{3}) + NI \cdot \sum_{n=2}^{\infty} \cos(n\theta - \varphi_B(n)) \\ MMF_C(\theta) = NI \cdot \cos(\theta - \frac{4\pi}{3}) + NI \cdot \sum_{n=2}^{\infty} \cos(n\theta - \varphi_C(n)) \end{cases} \quad (2)$$

Then, the magnetic flux ϕ produced will be:

$$\phi(\theta) = \frac{MMF_A(\theta) + MMF_B(\theta) + MMF_C(\theta)}{\mathfrak{R}} \quad (3)$$

And finally, if the current is homopolar (all phases fed with the same current):

$$\phi_0(\theta) = \frac{NI}{\mathfrak{R}} \cdot \sum_{n=1}^{\infty} \cos(3n\theta - \varphi(3n)) \Leftrightarrow L_0(\theta) = \frac{N \cdot \phi_0(\theta)}{I} \Rightarrow L_0(\theta) = \frac{N^2}{\mathfrak{R}} \cdot \sum_{n=1}^{\infty} \cos(3n\theta - \varphi(3n)) \quad (4)$$

As a consequence, the zero-sequence inductance results from the harmonics (mechanical reference) order multiple of 3.

Ultimately, the ideal harmonic spectra of the winding function can be resumed to three requirements. Firstly, the fundamental component would be the higher possible as the torque density will be. Secondly, all other harmonics with the exception of harmonics multiple of three, will be as low as possible. And lastly, with a preference for subharmonics and not the 3rd electrical component order, harmonics multiple of 3 will be as high as possible in order to obtain a high zero-sequence inductance.

Considering these criteria, a fast evaluation of the three machines can be performed. Then, analyzing the harmonic spectrum of the 12/8 machine in Fig.3 b) with the mechanical reference, it can be firstly observed that the 4th order mech. component corresponding to the electrical fundamental has the greatest value. However, it still traduces a low value of the winding factor for the fundamental of 0.75.

In addition, sub-harmonics as the 2nd order mech. harmonic are quite elevated and eddy-current losses can be predicted. Again, this harmonic rotates at a speed of $-\omega/2$ and the rotor rotates with an angular velocity of $+\omega/4$. Consequently, the MMF wave created in the magnets inside the rotor will be at a speed of $\omega/4 + \omega/2$ equals to $3\omega/4$ and will have two periods (2nd order). This means that the 2nd order harmonic will induce MMF waves in the magnets with a frequency corresponding to the 6th order harmonic. Generalizing this reasoning to all subharmonics, it is proven that all the MMF waves induced in the magnets located in the rotor are multiple of 3.

Table II: Fast analysis of the three machines with the winding function

Machine $N_s/2p$	12/8	12/10	18/10
Winding factors of the 1 st , 3 rd , 5 th and 7 th electrical harmonics	0.75 0 0.75 0.75	0.933 0.5 0.067 0.067	0.0945 0.577 0.14 0.061
Torque density (1 st elec. comp.)	Low	High	High
Torque ripple (5 th and 7 th elec. comp.)	High	Low	Low
Main harmonics of the EMF induced	5 th and 7 th	3 rd	3 rd
Main harmonics source of eddy-current losses in the magnets (mech. reference)	2 nd and 10 th	1 st and 7 th	1 st , 7 th and 13 th
Main MMF harmonics induced in the magnets	6 th	6 th and 12 th	6 th , 12 th and 18 th
Eddy-current losses in the magnets	High	High	Low

Lastly, harmonics multiple of 3 as the 6th, 18th and 30th order harmonics are not source of MMF since the topology is three-phase and the current has a sinus waveform. On the other hand, these harmonics allow swiftly revealing the presence of zero-sequence inductance. 3rd order electrical component is equal to zero but 5th and 7th order components are quite important and ripple torque can be expected.

Analyzes is also performed for the two other machines. Table II resumes the considerations for each machine that have been taken from their winding functions.

2.4 Zero-sequence inductance

As demonstrated in [9], the ratio between the homopolar inductance and the self inductance could be rapidly and precisely estimated. The calculation is done with those assumptions:

- The machine has no magnetic leakage
- The reluctance of the magnetic material of the stator and the reluctance of the rotor are negligible compared to the non-magnetic material (air)
- The air gap is constant

The method presented is based on the calculation of the air gap energy when only one phase is fed, traducing the self inductance, and when all phases are fed with the same current. This is the zero-sequence energy.

$$\begin{cases} E_s = \frac{1}{2} L_s \cdot I^2 \\ E_0 = \frac{3}{2} L_0 \cdot I^2 \end{cases} \Rightarrow \frac{L_0}{L_s} = \frac{1}{3} \frac{E_0}{E_s} \quad (5)$$

Then, with the developed expression of the energy, the inductance ratio becomes:

$$E = \frac{\Re}{2} \sum_{n=1}^N \phi^2 \Rightarrow \frac{L_0}{L_s} = \frac{1}{3} \frac{\sum_{n=1}^N \phi_0^2}{\sum_{n=1}^N \phi_s^2} \quad (6)$$

In order to calculate this inductance ratio, we need first to determine the MMF distribution, the air gap flux and then the air gap energy. Given that the air gap flux is the image of the MMF, these different steps could be easily done by graphically counting the surface of the piecewise waveforms [9] for the two cases. Figure 6 gives the instance for the machine 18/10:

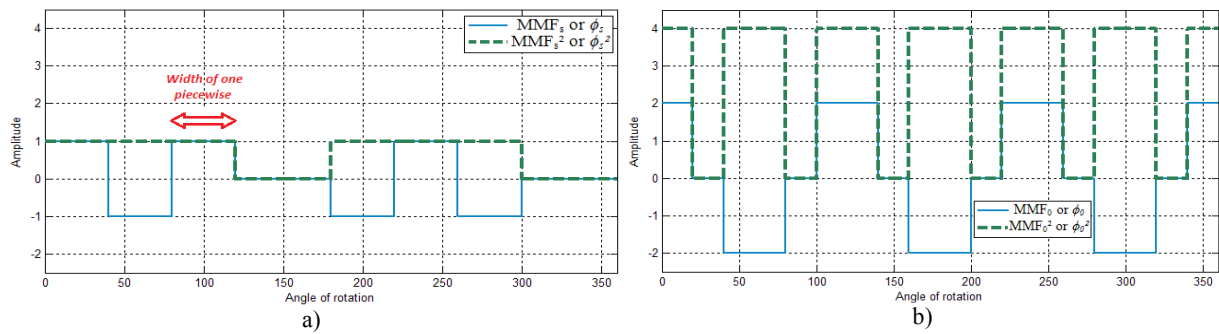


Fig. 6: Waveform of the air gap flux for the two cases: a) one phase fed and b) all phases fed

The calculation of the inductance ratio turns into:

$$\frac{L_0}{L_s} = \frac{1}{3} \frac{\sum_{n=1}^N \phi_0^2}{\sum_{n=1}^N \phi_s^2} = \frac{1}{3} \cdot \frac{6 \cdot 4}{6 \cdot 1} = \frac{4}{3} \approx 1.33 \quad (8)$$

Table III shows the value of the zero-sequence ratio for the three machines. It can be observed that the ratio for the machines 12/8 and 12/10 is equal to unit, meaning that there is no mutual between the phases. For the 18/10, the mutual is not null but positive. It involves a higher homopolar inductance.

Table III: Zero-sequence inductance ratio for the three machines

Machine $N_s/2p$	12/8	12/10	18/10
L_0/L_s	1	1	1.33

3 Simulation and performance analysis with FEA

Thanks to first assessment, designers have the possibility to get quickly a first idea about the behavior and the performance of the machines without employment of long simulations. However, the results obtained are approximated and more precise characterizations of machines are required. In this context, the three machines of this study have been simulated with *Flux2D* which is a FEA software. As known, FEA allows simulating the complete performance of the machines and evaluating very precisely the characteristics of the machines. Then the results obtained for the simulation are represented in the following tables:

Table IV: Inductances value of the three machines

Machine $N_s/2p$	L_0 (mH)	L_s (mH)	M (mH)	L_d (mH)	L_q (mH)
12/8	10.59	9.76	+ 0.4	10.67	8.39
12/10	8.46	9.35	- 0.43	9.92	9.66
18/10	12.43	11.07	+ 0.79	12.13	8.38

Table V: Performance of the machines at 1,500 rpm and 63.6 A RMS

Machine $N_s/2p$	Torque		Back-Emf				Eddy-current losses in the magnets (W)
	Mean torque (N.m)	Ripple torque (%)	1 st harmonic (V)	3 rd harmonic (%)	5 th harmonic (%)	7 th harmonic (%)	
12/8	170.4	6.4	371	18.5	10.4	2	178
12/10	212	0.7	508	13.5	1.9	2.7	540
18/10	235.6	0.5	496	33	4.2	0.9	38

Table VI: Performance of the machines at 12,000 rpm and torque of 35 N.m

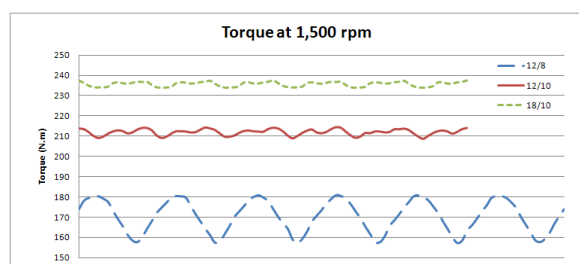
Machine $N_s/2p$	RMS Current (A)	Torque	Back-Emf				Eddy-current losses in the magnets (W)
		Ripple torque (%)	1 st harmonic = Bus voltage (V)	3 rd harmonic (%)	5 th harmonic (%)	7 th harmonic (%)	
12/8	31.8	44.4	800	7.3	47	10	3484
12/10	30	3.9	800	19	3.8	0.8	2400
18/10	31.4	1.3	800	111.2	3.7	1.1	570

Table VII: Iron and eddy-current losses of the machines at 1,500 rpm and 63.6 A RMS

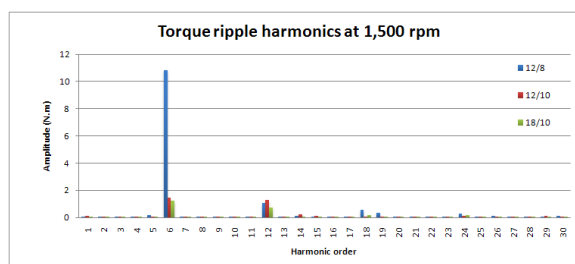
Machine $N_s/2p$	Rotor iron losses	Stator iron losses	Stator + rotor iron losses	Eddy-current losses in the magnets	Total Iron + eddy-current losses
12/8	53.7	126.3	180	178	358
12/10	61.5	154.4	215.9	540	755.9
18/10	53.2	195.1	248.3	38	286.3

Table VIII: Iron and eddy-current losses of the machines at 12,000 rpm and 35 N.m

Machine $N_s/2p$	Rotor iron losses	Stator iron losses	Stator + rotor iron losses	Eddy-current losses in the magnets	Total Iron + eddy-current losses
12/8	257.8	643	900.8	3484	4384
12/10	156.7	390	546.7	2400	2946.7
18/10	252.4	857	1109.4	570	1679.4



a)



b)

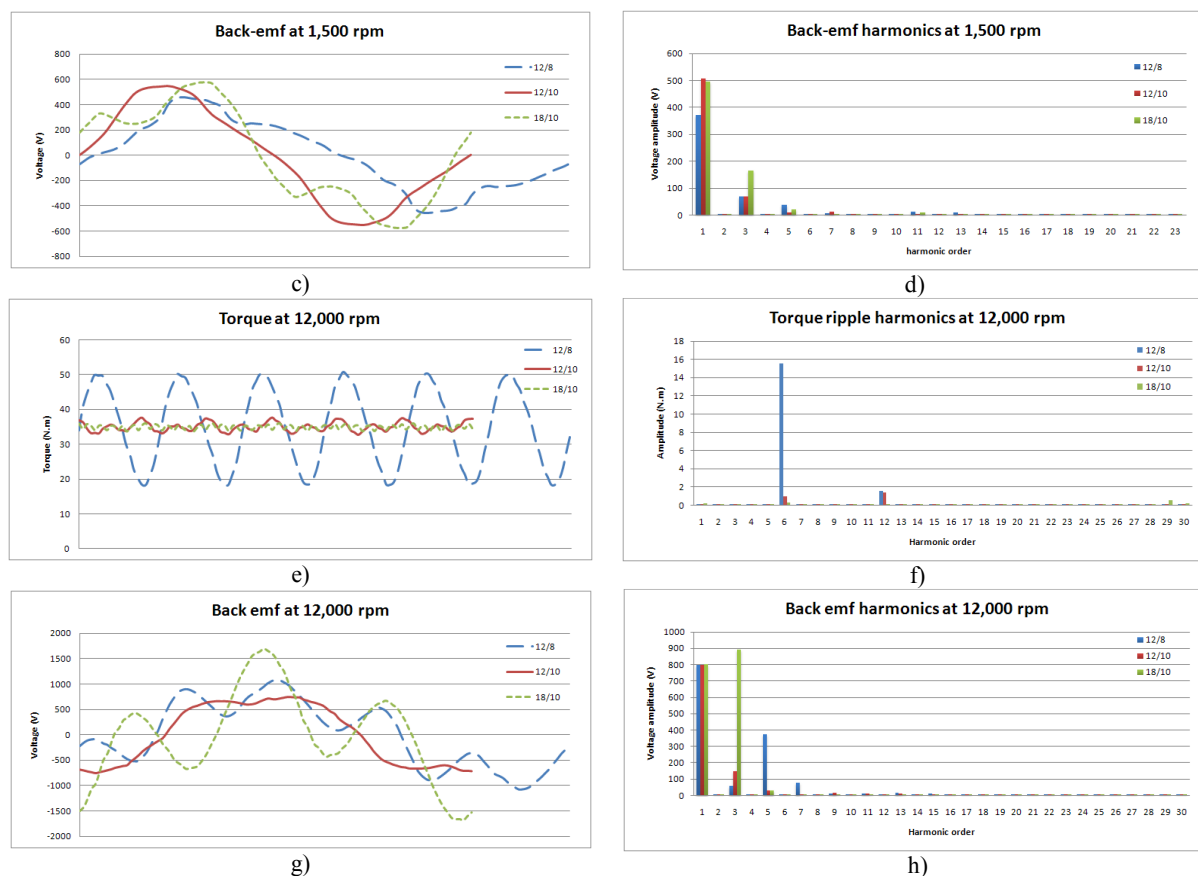


Fig. 7: Performances of the machines: at 1,500 rpm: a) Torque, b) Torque ripple, c) Back-emf and d) Back-emf harmonics; and at 12,000 rpm: e) Torque, f) Torque ripple, g) Back-emf and h) Back-emf harmonics

4 Discussions

Regarding the results obtained with FEA, comparison of the three machines and several deductions could be done more precisely:

- Firstly, the three machines have a high value of the homopolar inductance and low value of the mutual inductance. However, the 18/10 has a higher mutual inductance but also a higher homopolar inductance. In addition, the 12/8 and 12/10 have the advantage that the separation between phases is not only magnetic but also electric.
- Considering the torque produced, the 12/8 has a too low value of the mean torque due to its low value of the fundamental winding factor. Moreover, its torque ripple attains high value especially at 12,000 rpm. For the two other machines, the torque ripple is very low and the mean torque is high. The 18/10 produces a higher torque than the 12/10. This difference is much due to the reluctance torque available for the 18/10 which can be deduced from the values of the d-axis and q-axis inductances.
- For the back-emf, the 12/10 has the closest signal to the sinus form and has low values of harmonics. For the 12/8, harmonics are not very high at low speed but the 5th harmonic which is harmful to the drive control reach high values at high speed. The 18/10 has very elevated value of the 3rd harmonic mainly at high speed. This harmonic leads to homopolar currents on the electronic part and induce extra losses.
- Finally, comparing the iron plus the eddy-current losses of the machines, the best and lowest losses are for the 18/10. Due to the high value of the subharmonics, the 12/8 and 12/10 obtain very high value of eddy-current losses in the magnets. At 12,000 rpm, the losses are irremediable and conduct to the destruction of the magnets. One method to diminish these losses is to segment the magnets as the lamination of the iron part of the machine. The number of segmentation differs to the value of losses that has to be attained. In this study, the losses

have to not exceed around 400 W in the rotor part. Then, the segmentation could be realized along the axial direction and also in the radial direction.

Conclusively, the best choice seems to be the 18/10 machine. Its benefits concern mostly the high value of the torque density, the homopolar inductance and the low values of the total losses. However, some efforts should be fulfilled. Firstly, the too high value of the 3rd harmonic could be strongly reduced by skewing the rotor or the stator. Skewing continuously is not simple for the production and could be expensive. Thus, discrete skewing, eg. 5 steps skewing, is generally favored since the results are sufficient [5]. Lastly, the value of the eddy-current losses in the magnets could be lessened to a sufficient value by segmenting the magnets.

Conclusion

Owing to the use of a particular electric drive, the zero-sequence inductance has been introduced in the specifications of the machine to be designed. Afterward, three machines possessing a high zero-sequence inductance have been compared in order to determine the best solution for this EV application. In a first part, the performances of the machines have been estimated with an analytical approach which allows getting quickly an estimation of the homopolar inductance, the torque ripple and the main characteristics. Then, the comparison of the three machines has been involved with the employment of FEA. Finally, the results obtained permit to evaluate and choose the best machine but to also confirm the assessment of the analytical methodology.

References

- [1] M. Barcaro and al., Performance evaluation of an integrated starter alternator using an interior permanent magnet machine, *IET Electr. Power Appl.*, vol.4, Iss. 1, pp.539-546, 2010.
- [2] Liu Qinghua and al., Design optimization of interior permanent magnet synchronous motors for wide-speed operation, *IEEE Power Electronics and Drive Systems Conference, PEDS'01*, Bali, Indonesia, Oct. 2001
- [3] N. Bianchi and al., Design considerations for fractional-slot winding configurations of synchronous machines, *IEEE Trans. On Ind. Appl.*, vol. 42, No. 4, Jul./Aug. 2006
- [4] M. T. Abolhassani and H. A. Toliyat, Fault Tolerant Permanent Magnet Motor Drives for Electric Vehicles, *IEEE Int. Electric Machines and Drives Conference, IEMDC'09*, Miami, USA, May 2009
- [5] G. Dajaku and D. Gerling, Skewing Effect on the PM Flux-Linkage High Harmonics of the PM Machine with Delta Winding, *IEEE Power Electronics and Appl. Conf., EPE'09*, Barcelona, Spain, Sept. 2009
- [6] L. De-Sousa, B. Silvestre and B. Bouchez, A combined Multiphase Electric Drive and Fast Battery Charger for Electric Vehicles, *IEEE Vehicle Power and Propulsion Conference, VPPC'10*, Lille, France, Sept. 2010
- [7] L. De-Sousa, B. Bouchez, Combined Electric Device for Powering and Charging, *International Patent WO 2010/057892 A1*
- [8] A. Bruyère and al., A Multiphase Traction/Fast-Battery-Charger Drive for Electric or Plug-in Hybrid Vehicles, *IEEE Vehicle Power and Propulsion Conference, VPPC'10*, Lille, France, Sept. 2010
- [9] L. De Sousa and H. Dogan, Method of evaluating the zero-sequence inductance ratio for electrical machines, *IEEE Power Electronics and Appl. Conf., EPE'11*, Birmingham, UK, Aug./Sept. 2011
- [10] J. A. Güemes and al., Comparative Study of PMSM with Integer-slot and Fractional-slot Windings, *IEEE International Conference on Electrical Machines, ICEM'10*, Rome, Sept. 2010
- [11] F. Magnussen and H. Lendenmann, Parasitic Effects in PM Machines With Concentrated Windings, *IEEE Trans. On Ind. Appl.*, vol. 43, No. 5, Sept./Oct. 2007
- [12] N. Bianchi and M. Dai Pré, Use of the star of slots in designing fractional-slot single-layer synchronous motors, *IEE Proc.-Electr. Power Appl.*, Vol. 153, No. 3, pp. 459-466, May 2006
- [13] G. Ugalde and al., Space Harmonic Modeling of Fractional Permanent Magnet Machines from Star of Slots, *IEEE Electrical Machines Conference, ICEM'08*, Vilamoura, Portugal, Sept. 2008
- [14] J. T. Chen and Z. Q. Zhu, Winding Configurations and Optimal Stator and Rotor Pole Combination of Flux-Switching PM Brushless AC Machines, *IEEE Trans. On Energy Conv.*, vol. 25, No. 2, June 2010
- [15] N. Bianchi and al., A General Approach to Determine the Rotor Losses in Three-Phase Fractional-Slot PM Machines, *IEEE Int. Conf. On Electric Machines & Drives, IEMDC'07*, Antalya, May 2007